Heliyon 9 (2023) e13133

Contents lists available at ScienceDirect

Heliyon

journal homepage: www.cell.com/heliyon

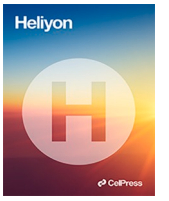

Research article

Characterization of aspartokinase double mutants using a combination of experiments and simulations

Zhijie Chen [b,1], Yu Fu [a,1], Shimeng Liu [c], Xinyu Huang [a], Xiaoting Kong [a], Zhaojie Mao [a], Ning Hu [a], Fengxiang Zhang [a,**], Caijing Han [a,*]

[a] School of Public Health, Weifang Medical University, Weifang, 261053, Shandong, China
[b] School of Pharmaceutical Sciences, Tsinghua University, 100084, Beijing, China
[c] Jiaxing Xinbeilai Biotechnology Co., Ltd, China

ARTICLE INFO

Keywords:
Aspartokinase
Double mutant
Site-directed mutation
MST
MD
Mechanism

ABSTRACT

Aspartokinase (AK) is synergistically suppressed by Thr and Lys in the *Corynebacterium* metabolic pathway. Site-directed mutations can significantly improve AK inhibition. Our previous studies confirmed that sites 379 and 380 were important sites affecting enzyme activity, so we further screen the double mutants with excellent enzymatic properties from sites 379 and 380, and discuss the difference of enzyme activity between the double mutants and single mutants. Here, a double mutant, T379L/A380 M, with improved enzyme activity (2.74-fold) was obtained. Enzymatic property experiments showed that the optimum temperature of T379L/A380 M increased from 26 °C (recombinant *Escherichia coli*; WT-AK) to 45 °C and that the optimal pH decreased from 8.0 (WT-AK) to 7.5. Further, the half-life decreased from 4.5 to 3.32 h. These enzymatic properties were better than other mutant strains. Inhibition was diminished with low concentrations of Lys, and Lys + Thr presented an activating role. Subsequently, the reasons for the improved AK enzyme activity were illustrated with microscale thermophoresis (MST) experiments and molecular dynamic (MD) simulation by measuring ligand affinity and AK conformational changes. MST showed that the affinity between T379L/A380 M and Lys decreased, but the affinity between T379L/A380 M and Asp increased, promoting T379L/A380 M enzyme activity. MD experiments showed that T379L/A380 M enhanced the Asp-ATP affinity and catalyzed the transfer of residues S192 and D193 to Asp, promoting T379L/A380 M enzyme activity. However, the mutation did not cause fluctuations in the substrate Asp and ATP pockets. This might be why the enzyme activity was inferior to that of the single mutants (T379L and A380 M).

1. Introduction

Methionine, as the only sulfur-containing essential amino acid, can only be acquired from food and cannot be synthesized in the human body. Currently, it is generally produced via chemical synthesis, resulting in marked environmental pollution. Methionine is

* Corresponding author.
** Corresponding author.
E-mail addresses: zfx0515@163.com (F. Zhang), hancaijing@wfmc.edu.cn (C. Han).
[1] These authors contributed equally to this work.

https://doi.org/10.1016/j.heliyon.2023.e13133
Received 6 August 2022; Received in revised form 14 January 2023; Accepted 18 January 2023
Available online 28 January 2023

inhibited by a variety of enzymes involved in microbial fermentation, leading to lower yields [1]. Aspartokinase (AK) as the first key allosteric enzyme in the metabolic pathway of *Corynebacterium pekinensis* is regulated by feedback inhibition by metabolic branch products. It can flexibly control the carbon flow and reaction speed according to the concentration of end products, in order to control the output of downstream metabolites (lysine, threonine, aspartic acid, and methionine) [2]. Therefore, the modification of AK is of great significance to improve the output of downstream metabolites. Site-directed mutation plays an important role in generating recombinant proteins; For example, Yang et al. reported that the mutants E334D, E334F, and E334R of 5-carboxy-2-pentenoyl-CoA reductase could be obtained by mutating the enzyme active site, resulting in much higher enzymatic activity than that of the wild-type enzyme [3]. Ali reported that a mutant of New Delhi metallo β-lactamase-1 (NDM-1) could be generated by PCR-based site-directed mutagenesis, replacing Q with A at the non-active site 123 (NDM-1^{Q123A}), resulting in enhanced hydrolytic activity (Kcat/Km), as compared to that of wild-type NDM-1 [4]. Therefore, site-directed mutagenesis is of great significance for protein modification.

AK is currently known as a polymeric allosteric enzyme in the form of a heterotetramer ($\alpha_2\beta_2$), present in organisms such as *Corynebacterium glutamicum* [5], thermophilic bacteria [6], and *Mycobacterium tuberculosis* [7]. Both *Escherichia coli* and *Arabidopsis* AK are homooligomers [7], and AK in cyanobacteria is a heterodimer (αβ) [8]. *C. glutamicum* AK (CgAK) is a typical allosteric enzyme, which is inhibited by the synergistic feedback originated from lysine and threonine [9]. The binding sites of the inhibitor lysine are the ACT1 (14–93) (β-subunit) and ACT2 (250–262, 343–409) (α-subunit); The binding sites of the inhibitor threonine are ACT1 (253–342) and ACT2 (250–262, 343–409) of the α subunit and ACT1 (14–93) and ACT2 (1–13, 94–160) of the β subunit. Inhibitor binding will lead to a change in the conformation of the enzyme, which is not conducive to substrate binding, resulting in the inhibitory effect. Lysine and threonine, as allosteric inhibitors of AK, regulate the binding strength with the substrate through allosteric regulation, to affect carbon flow of the metabolic pathway. CpAK exists as a monomer and is still regulated by the allosteric effects of lysine and threonine [10]. The monomer AK can also regulate downstream metabolites through allosteric regulation. Therefore, in a previous study, AK was modified to obtain a mutant in which feedback inhibition was relieved and enzyme activity was improved, and the mechanism through which enzyme activity increased was described [10,11]. However, with the progression of microbial fermentation, acid and heat will eventually be produced, resulting in a decrease in the pH and an increase in the temperature. Therefore, improvements to the optimal temperature and pH of the enzyme will greatly reduce the energy consumption in the fermentation process and play an important role in improving processes related to downstream metabolites.

In a previous study, we found that site 379 can associate with Lys through two hydrogen bonds and that site 380 can bind Lys through a water bridge, indicating that they are important residues for Lys. The single mutants A380I, T379L, and A380 M and double mutant T379 N/A380C were obtained by inducing saturation mutations and high-throughput screening, and the enzyme activity was improved; however, enzymatic properties were not improved. Our previous studies confirmed that sites 379 and 380 are important sites affecting enzyme activity [12,13]. In this study, we used sites 379 and 380 as saturated mutation sites (Fig. 1), generated double mutations based on these sites, and obtained the double mutant T379L/A380 M with improved enzyme activity (than WT-AK) and enzymological properties through screening. However, the activity of T379L/A380 M was decreased compared with that of the single mutant (T379L and A380 M). To reveal the reasons for the enzyme activity and enzymological properties, microscale thermophoresis (MST) was performed and circular dichroism (CD) and molecular dynamic (MD) spectra were investigated. In the discussion, we compared the possible reasons why the enzyme activity of the double mutant T379L/A380 M was inferior to that of the single mutant (T379L and A380 M).

2. Materials and methods

2.1. Experimental materials

WT-AK was preserved in our laboratory, Ni Sepharose™ 6 Fast Flow was purchased from General Electric Company (Fairfield, CT,

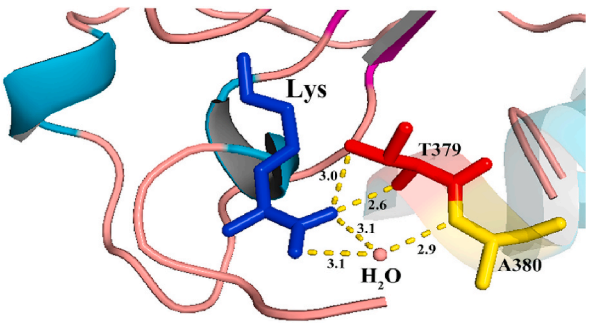

Fig. 1. Selection Basis. Blue was inhibitor lysine. Red is 379 site. Yellow was 380 site. The 379 site was connected to the inhibitor Lys by two hydrogen bonds, whose distance was 3.0 Å and 2.6 Å, respectively. The 380 site was connected to the inhibitor Lys by a water bridge, whose distance was 2.9 Å, 3.1 Å and 3.1 Å, respectively. (For interpretation of the references to colour in this figure legend, the reader is referred to the Web version of this article.)

USA), and His-Tag (27E8) Mouse mAb (HRP Conjugate; Art. No. 9991S) was purchased from Cell Signaling Technology (Boston, MA, USA). The Monolith™ Protein Labeling Kit RED-NHS and Capillaries for the Monolith NT115 Standard Capillary were purchased from NanoTemper Technology Co., Ltd. (Beijing, China).

2.2. Construction of mutant strains

With the extracted plasmid as a template, the target gene was amplified by PCR using primers harboring the mutation (T379L/A380 M 5′-CAGAGCTTCCATGAACTCNNNNNNAACACCTGGGTGAG-3′ and 5′-CAGTCTCACCCAGGTGTTNNNNNNGAGTTCATGGAAGC-3′), and the methylated template was digested with *Dpn*I enzyme after being verified by 1% agarose nucleic acid electrophoresis. Subsequently, the digested product (1.2 μL) was added to *E. coli* BL21 receptors (100 μL) by ice bath (5 min), heating (42 °C for 90 s), again ice bath (2 min). Then, it was added to 900 μL of LB without antibiotics, cultured at 37 °C for 90 min with 160–170 rpm of shaking, and centrifuged. Next, 800 μL of culture medium was discarded, and the bacteria were mixed evenly with the remaining 100uL medium. Then They were spread the solid plates containing kanamycin to screen a monoclonal antibody. After the monoclonal antibody was cultured, its bacterial solution was used as template, the target gene was amplified by PCR using the cloning primers and then sequenced after preliminary verification via 1% agarose nucleic acid electrophoresis.

2.3. Purification and validation

After sequencing, the engineered bacteria were subjected to culture and induced with IPTG (Isopropyl-β-D-Thiogalactoside) at 23 °C overnight. The bacteria were collected by centrifugation at 8000 rpm at 4 °C for 10 min and then re-suspended by adding 10 mL of PBS (pH 7.4). After ultrasonic fragmentation, the crude enzyme solution was centrifuged at 8000 rpm at 4 °C for 10 min. The purified method was as follows: The Ni Sepharose™ 6 Fast Flow column was balanced with 20 nM imidazole, then the impurity proteins were removed with 20 mM, 40 mM, 70 mM, 100 mM and 200 mM imidazole buffers and finally the target proteins were eluted with 500 mM imidazole buffers.

2.4. Characterization of mutant strains

Kinetic determination: The reaction system (1 mL) was as follows: 1.6 mM $MgSO_4$, 10 mM L-Asp, 800 mM KCl, 10.4 mM ATP (in 25 mM tris-HCl), 800 mM NH_4OH, 10 mM β-mercaptoethanol and 100 mM tris-HCl buffer solution (pH 8.0). The purified enzyme (50 μL) and different concentrations of L-Asp (0–16 mM) were added to the reaction at 28 °C for 30 min, and then, an equal volume of $FeCl_3$ (dissolved in 0.1 M HCl, 12% trichloroacetic acid, and 3 M HCl at a volume ratio of 1:1:1) was added to terminate the reaction, before measuring the absorbance at 540 nm. The nonlinear equation was fitted with the Hill equation using Origin 8.5 software (Northampton, MA, USA, Origin Lab), as follows: $V = Vmax\ (Sn)/(Kn + Sn)$.

Optimum temperature: The reaction process is shown previously herein, but the reaction was induced based on different temperature gradients (15–50 °C) for 30 min. Water was used to replace the substrate, and the highest enzyme activity was defined as 100%.

Optimum pH: The reaction process is shown previously herein, but the reaction proceeded based on different pH gradients (7.0–9.0) for 30 min.

Enzyme stability: Purified enzyme solution was added to the reaction system at the optimum temperature and pH for 30 min. The enzyme activity measured at this time was defined as 100%, and then, it was measured every hour, 10 times. The time taken for the enzyme activity to drop to half of the initial enzyme activity was considered the half-life.

Substrate inhibitor: The purified enzyme solution (20 μL) and 0–10 mM of inhibitor (Lys, Thr, Met, Lys + Thr, Lys + Met, Thr + Met, Lys + Thr + Met) were added to a 180 μL reaction system at 28 °C for 30 min, and then, an equal volume of $FeCl_3$ was added to stop the reaction.

The results were reported as mean ± standard deviation (SD), and analyzed by ANOVA-multiple comparisons. *P*-values <0.05 or <0.01 were considered statistically significant.

2.5. Microscale thermophoresis analysis [13]

MST was performed according to the instructions of the kit (MO-X001). The main steps were as follows[13]: The concentration of purified AK was adjusted to 2–20 mM with labeled buffer. The dissolved fluorescent dye (NT-647-NHS) was adjusted to 2–3 folds of the protein concentration with the marker buffer. The protein and fluorescent dye were mixed 1:1 for dark reaction 30 min, and then purified according to the purification kit operation. The ligands (Asp and Lys) were dissolved in a reaction system and incubated with the labeled protein (40 nM) at room temperature for 10 min. Then the dissociation constant (Kd) was measured by Nano Temper Technologies.

2.6. Molecular dynamic simulation [11]

The simulation was carried out according to a previously reported method in the literature [11]. The main steps were as follows: AMBER 16 software was used in the MD simulation and the ff14SB force field acted on the protein. The energy in each system was minimized by the steepest-descent method and the conjugate gradient method. The particle mesh Ewald algorithm was used to

evaluate the long-range electrostatic interactions. The bond lengths of hydrogen atoms attached to heavy atoms was constrained the SHAKE algorithm during the simulations. The MM/GBSA module in AMBER16 was used to calculate the binding free energy between ATP and Asp. The per-residue decomposition scheme in the MMPBSA.py script conducted the binding free energy decomposition of all residues.

3. Results and discussion

3.1. Construction and purification of mutant strains

The recombinant plasmid consisted of pET-28a (5369 bp) and the target gene encoding AK (1266 bp), and thus, the extracted plasmid produced a band at 7000 bp by gel electrophoresis (Fig. S1A). With this plasmid as a template, PCR amplification was carried out using mutation-containing primers, and this also resulted in a target band at 7000 bp (Fig. S1B). PCR amplification was carried out using a mutant bacterial suspension as a template with the cloning primers, and the amplified AK-encoding gene resulted in a band at 1266 bp (Fig. S1C). The successfully sequenced strain showed induced AK expression, as indicated by a band at 48 kDa with SDS-PAGE and western blotting (Fig. S1D).

3.2. Analysis of kinetics and enzymatic properties

The kinetic parameters of recombinant *Escherichia coli* (WT-AK) and mutant strains are shown in Table 1. The maximum reaction rates of WT-AK and T379L/A380 M were 3.28 and 7.9 U/mg min^{-1}, respectively, indicating that enzyme activity increased by 2.74-fold with the mutation. The WT-AK n value was 1.54, showing positive synergy. For the double mutant T379L/A380 M, the n value was 1.74, which decreased synergistically. The Km value of WT-AK was 4.17, and this value decreased to 0.41 with the mutation, indicating increase in affinity.

Surprisingly, the optimal temperature of the mutant strain T379L/A380 M was 45 °C, markedly greater than that of WT-AK at 26 °C (Fig. 2B). The enzyme activity of the mutant strain decreased sharply at temperatures higher than the optimum temperature, but the enzyme activity was still higher than that of WT-AK at 50 °C, indicating that the high-temperature tolerance had improved with the mutation. Isogai reported that the mutant (Gly474Asp and Cys554Tyr variants) of AK/HSDH (a bifunctional aspartate kinase/homoserine dehydrogenase) conferred high-temperature stress tolerance to *E. coli* cells [14]. The conclusion of this paper was consistent with Isogai's report.

The mutant strain T379L/A380 M had a lower optimum pH 7.5 than that of WT-AK (optimum pH 8.0), which would be conducive to fermentation, because acid is produced during this process (Fig. 2C). The half-life of WT-AK was 4.5 h, whereas that of the mutant strain T379L/A380 M was slightly reduced to 3.32 h (Fig. 2D). WT-AK was inhibited by Lys, Thr and Met in a dose-dependent manner, as shown in Fig. 3. When only one inhibitor is present, the inhibitory effect was poor (approximately 10%) ($P < 0.01$). The inhibitory effect was further strengthened under the combined action of two inhibitors. Among them, the synergistic feedback inhibition mediated by Thr and Lys was strongest with a 65% inhibition rate ($P < 0.01$), which is consistent with literature reports [6]. When the three inhibitors were present at the same time, the inhibitory effect was strongest, reaching 70% ($P < 0.01$). With the mutation, the inhibitory effect was diminished to varying degrees, and lysine changed from having an inhibitory to activating effect at low concentrations ($P < 0.01$). The inhibitory effect also showed different degrees of attenuation under the combined action of the two inhibitors. Surprisingly, the combined action of Lys + Thr resulting in activation at a concentration of 1 or 5 mM, which was significantly different in the control group ($P < 0.01$). When the three inhibitors were present at the same time, the inhibitory effect was also significantly diminished within the experimental concentration range. It can be seen from Fig. 3 that all sites with an activation effect were determined to contain Lys. It is possible that position 379 is directly associated with Lys, and thus, the inhibition of Lys was most obvious after generating the mutation. Yoshida reported that Thr361 (CgAK) directly or indirectly participates in the effects of Lys, reducing the inhibitory effect of Lys owing to an effective mutation in the binding site, and thus, the conclusion of this article is consistent with a literature report [5].

3.3. MST experiment and CD spectrum

Inhibition or activation could be determined based on the different affinities between the enzyme and inhibitor. Therefore, we explored the affinity between the enzyme and the ligand on an experimental level. MST was used to test the affinity between the enzyme and the inhibitor (Fig. 4A). The Kd value is usually negatively correlated with affinity. The Kd value for WT-AK and Lys was 1.32 mM, and the Kd value for T379L/A380 M was increased to 5.43 mM, indicating that the affinity decreased in different extent. The mutation could effectively relieve the inhibitory effect of Lys, which was consistent with the results shown in Fig. 3. In the presence of 10 mM Lys, the Kd value of WT-AK-Lys + Asp was 701.25 mM, whereas the Kd value of T379L/A380M-Lys + Asp was 373.79 mM ($p <$

Table 1
Parameters of dynamics.

Strain	Vmax	Km	n	Fold
WTAK	3.28	4.77	1.54	
T379L/A380 M	9	0.41	1.74	2.74

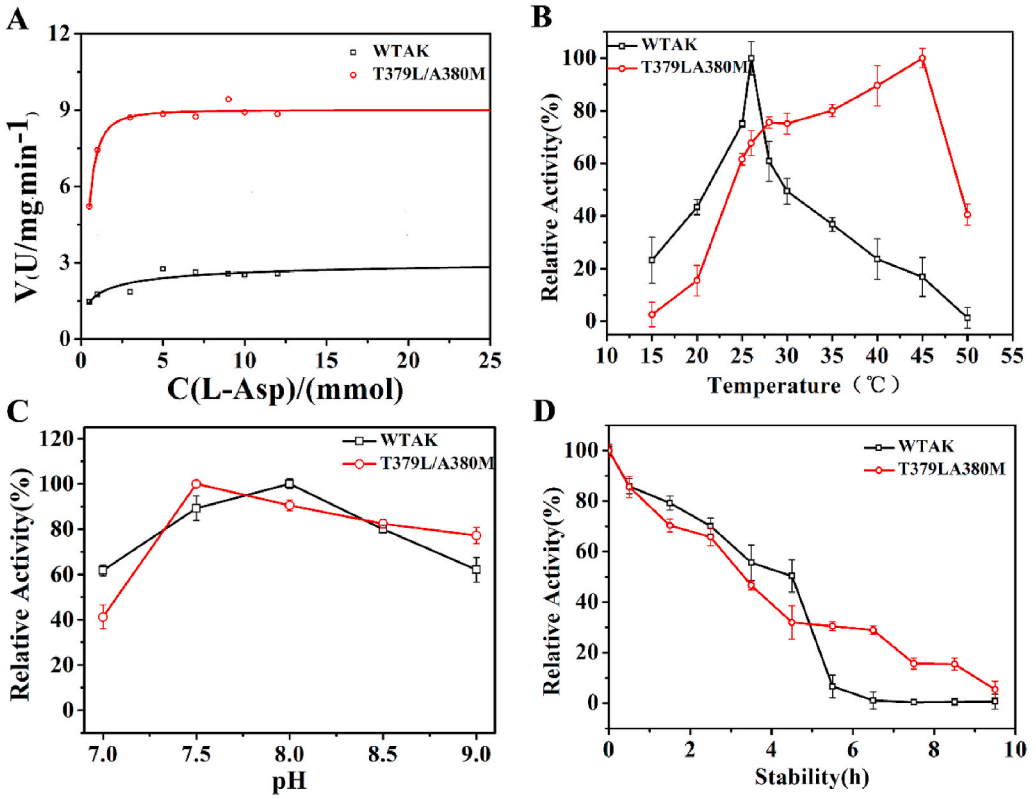

Fig. 2. Enzyme activity. A, Enzyme activity; red represented T379L/A380 M; black represented WTAK, the same below. B, optimum temperature; C, optimum pH; D, thermal stability. (For interpretation of the references to colour in this figure legend, the reader is referred to the Web version of this article.)

0.05), indicating that the affinity of T379L/A380 M for Asp increased when Lys was present (Fig. 4B), which was consistent with the results shown in Fig. 3B. This could be due to the decreased affinity for Lys and increased affinity for Asp after introducing the mutation. The Kd value of WT-AK + Asp was 655.86 mM, and that for T379L/A380 M was 152.12 mM (Fig. 4C). The affinity of the mutant strain for the substrate Asp was greater, which usually be indicated that it could easily react with Asp with the mutation, which was consistent with the results shown in Fig. 2A. The Kd values for WT-AK-Asp and WT-AK-Lys + Asp were 686.86 and 701.25 mM, respectively. Lys, as an inhibitor, could inhibit AK activity and decrease the affinity for Asp, which was consistent with data shown in Fig. 3 and previous literature [15]. The Kd value for T379L/A380M-Lys + Asp was 373.79 mM, indicating that the affinity between the mutant and the substrate Asp (373.79 mM) was greater than that with WT-AK (701.25 mM) in the presence of Lys. This could be due to the negative effect of mutations on the inhibitor effect of Lys, thus increasing the affinity for substrates. The changes in the secondary structure of WT and T379L/A380 M were observed by CD (Fig. 4D). The α-helix of T379L/A380 M was reduced to 13.4% (WT-AK 14.7%) in CD spectrum, indicating that the rigid structure of the enzyme was reduced and the enzyme was more flexible, so the stability of the enzyme would be reduced, which was consistent with the experimental data (Fig. 2D). We observed the proportion of each secondary structure in the simulation process. The α-helix of T379L/A380 M was reduced than WT-AK, whose trend was consistent with CD spectrum.

3.4. Analysis of MD simulation

In view of the aforementioned experimental results, we further used MD simulation for the two complex systems of WT-AK + Asp + ATP and T379L/A380 M + Asp + ATP to reveal the reasons for the variation in AK properties caused by mutations. The root mean square deviation (RMSD) curve was stable, indicating that the simulation was successful and could be used for subsequent analysis (Fig. 5A) [16]. The binding energy between T379L/A380 M and ATP was −14.34 kcal/mol, which was lower than that of WT-AK (−6.5 kcal/mol) in the 100 ns simulation process (Fig. 5B) [17]. Owing to the lower binding energy indicating stronger binding ability [18], T379L/A380 M had stronger binding affinity for ATP than WT-AK. Similarly, the binding energy of T379L/A380 M to Asp was −14.82 kcal/mol, indicating that the binding affinity for substrate Asp was stronger than that of WT-AK (−10.53 kcal/mol). After introducing the mutation, the binding force with ATP and Asp was enhanced, which would be conducive to improving the enzyme activity of the mutant; this was consistent with the experimental results shown in Fig. 2A. It can be seen from Fig. 5C that the distance between ATP and Asp became closer in the 100 ns simulation, which was conducive to the transfer of pi in the catalytic reaction, to

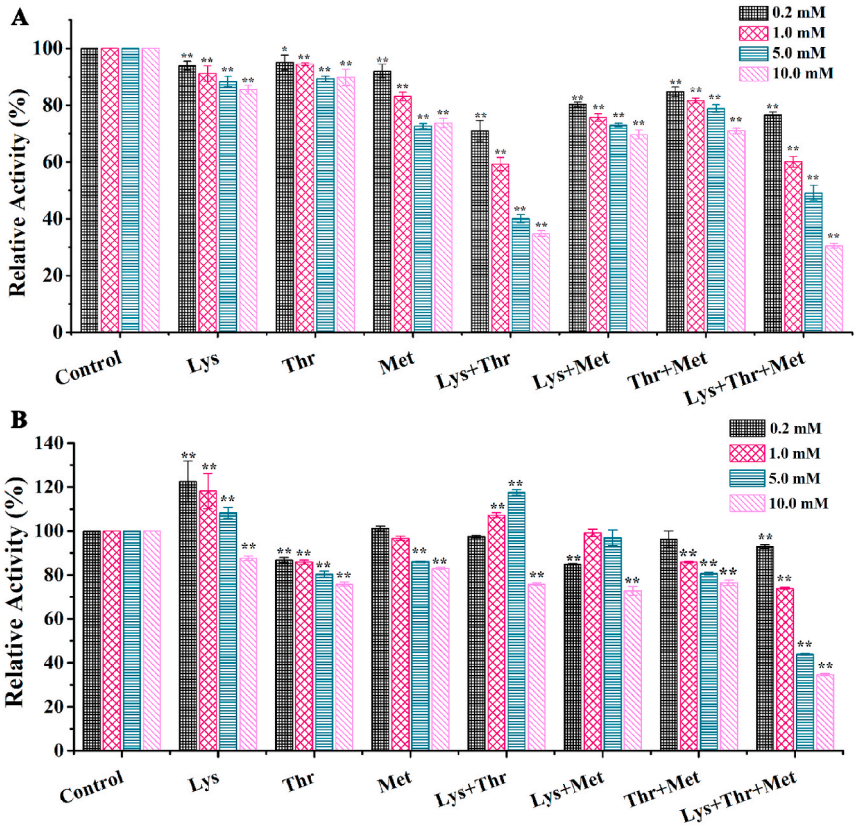

Fig. 3. Relative enzyme activity of WTAK and T379L/A380 M under different substrate inhibitor conditions. A, Relative enzyme activity of WTAK; B, Relative enzyme activity of T379L/A380 M; All experiments were performed in triplicate, n = 3; $^{*}P < 0.05$ versus the control group. $^{**}P < 0.01$ versus the control group.

accelerate the catalytic reaction rate. In the first 55 s of the simulation, the distance between ATP and Asp of T379L/A380 M was slightly larger than that for WT-AK, but in the later simulation, ATP and Asp of T379L/A380 M gradually approached each other, and the distance was significantly smaller than that of WT-AK. In the simulation process, T379L/A380 M appeared to have two maximum probabilities, and the probability at a distance of 0.85 nm was 0.17, which was significantly higher than that (0.13) at a distance of 1.45 nm, indicating that the distance between ATP and Asp for T379L/A380 M was mainly 0.85 nm. However, the probability with WT-AK was 0.234 at 1.25 nm, which was significantly higher than that of T379L/A380 M. Thus, the distance between ATP and Asp of T379L/A380 M was less than that of WT-AK as a whole in the simulation process. In conclusion, T379L/A380 M has strong binding affinity for ATP and Asp, and the distance between them became closer, which might be one of the reasons for the increase in enzyme activity.

When AK was not bound to the inhibitor, AK-R was in a loose state, which was conducive to substrate binding. In the presence of Lys, AK-T, in a tight state, was not conducive to substrate binding owing to an obvious allosteric regulatory effect [19,20]. The conformation of the enzyme (T and R states) would affect the binding of the enzyme to the substrate. Therefore, the conformational changes to WT-AK and T379L/A380 M were obtained in the simulation process (Fig. 6A, B, C). In the simulation process, the radius of gyration (Rg) of T379L/A380 M increased first and then decreased, indicating that its conformation has changed from R state to T state. The affinity between the R state and substrate was strong, which was conducive to improving the enzyme activity, but the affinity between the T state and substrate was weak, which was not conducive to improving the enzyme activity. This phenomenon was difficult to understand. Therefore, we also selected the PDB conformation at 100 ns. Surprisingly, the Asp of T379L/A380 M was close to the catalytic residues S192 and D193, which was conducive to catalysis (Fig. 6D). This reasonably explained the reason for decreased Rg after 40 ns and increased enzyme activity, which was also consistent with the enzyme property data (Fig. 2). In addition, the electrostatic potential around sites 379 and 380 changed from a positive charge to a negative charge after introducing the mutation, which might also be conducive to enhancing enzyme activity (Fig. 6A–B).

The solvent-accessible surface area (SASA) also increased at first (60 s) and then decreased (after 40 s) in the simulation process, and the inflection timepoint was consistent with the Rg (Fig. 6E). The larger SASA denoted a larger contact area between the enzyme and the solvent, indicating that the conformation of the enzyme was looser, increasing the contact surface between the residue and the solvent. In the first 60 s, the maximum probability of T379L/A380M-SASA (222 nm) was larger than that of WT-AK (217 nm), indicating that it had a good contact area with the solvent. Similarly, T379L/A380M-SASA (maximum probability, 216 nm) was

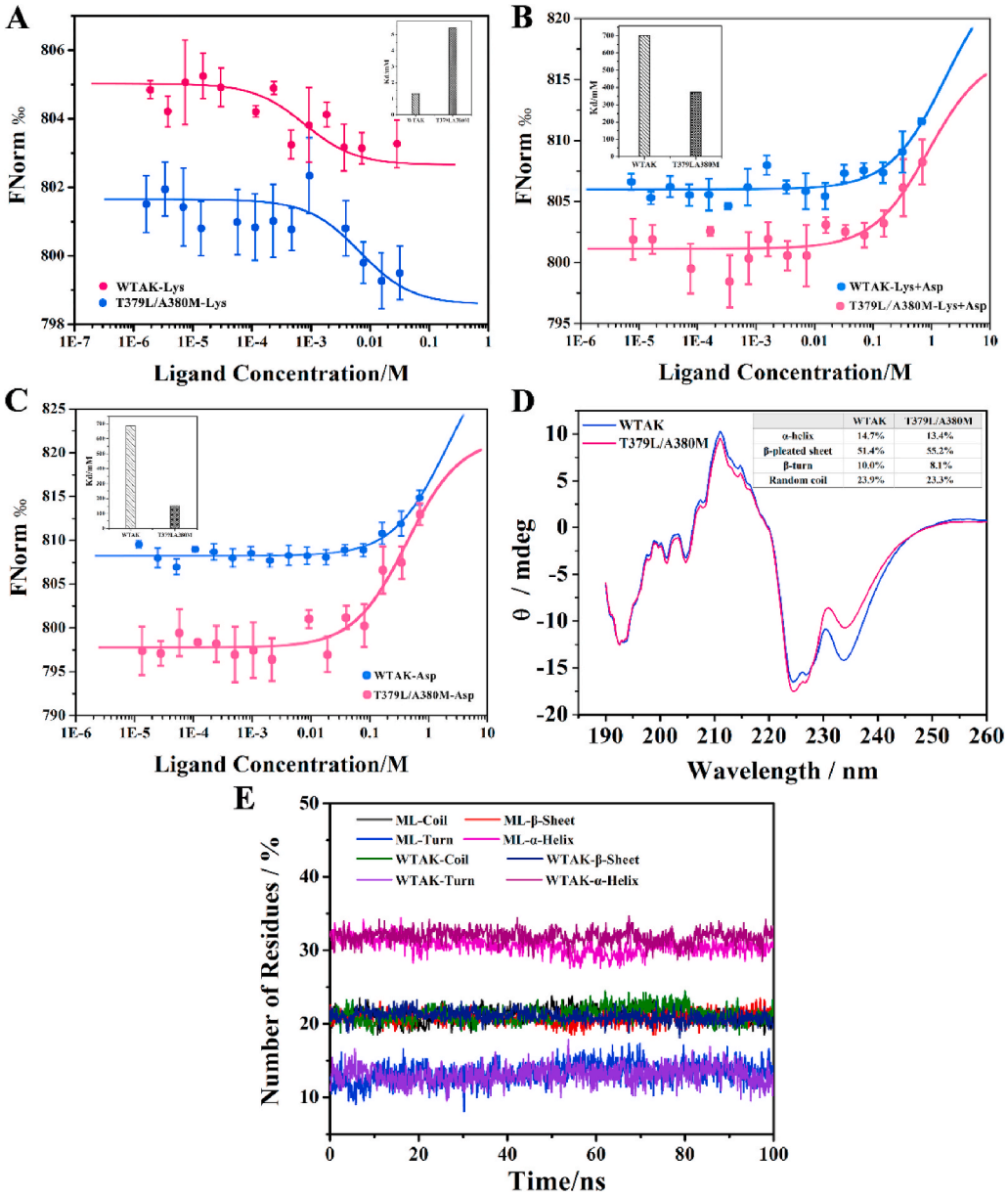

Fig. 4. MST, CD and MD. A, Affinity with Lys of WTAK and T379L/A380 M; Pink solid circle represented T379L/A380M-Lys; Blue solid circle represented WTAK-Lys, the same below. B, Affinity with Asp of WTAK and T379L/A380 M in the presence of Lys; Pink solid circle represented T379L/A380M-Lys + Asp; Blue solid circle represented WTAK-Lys + Asp. C, Affinity with Asp of WTAK and T379L/A380 M. Pink solid circle represented T379L/A380 M + Asp; Blue solid circle represented WTAK + Asp. D, Circular dichroism. E, Secondary structure changes during MD. (For interpretation of the references to colour in this figure legend, the reader is referred to the Web version of this article.)

smaller than that of WT-AK at 222 nm after 40 s, indicating that the conformation of the enzyme became tight and that the contact surface with the solvent was reduced (Fig. 6F–G). Therefore, the change in SASA values also indirectly explained the change of enzyme conformation from an R state to a T state, and the conformation change led to a change in enzyme activity.

Root Mean Square Fluctuation (RMSF) represented the flexibility of the residual, and it is very important to increase enzyme activity. The catalytic reaction of the enzyme comprised ATP transferring the third Pi to ADP and phosphorylating it to form Asp (Fig. 7A). Therefore, the flexibility of residues with respect to ATP and Asp attachment was determined to be crucial for enzyme activity. In a previous study, we discussed the reasons for the increase in enzyme activity with the single mutants T379L and A380 M, indicating that they had a common feature. Specifically, the fluctuation in RMSF and the ATP and Asp binding pocket causes increased enzyme activity. However, the enzyme activity of the double mutant T379L/A380 M, which we accidently obtained, did not correspond to this, and in contrast, it was decreased compared with that of the single mutant. Therefore, we tested the fluctuation in RMSF

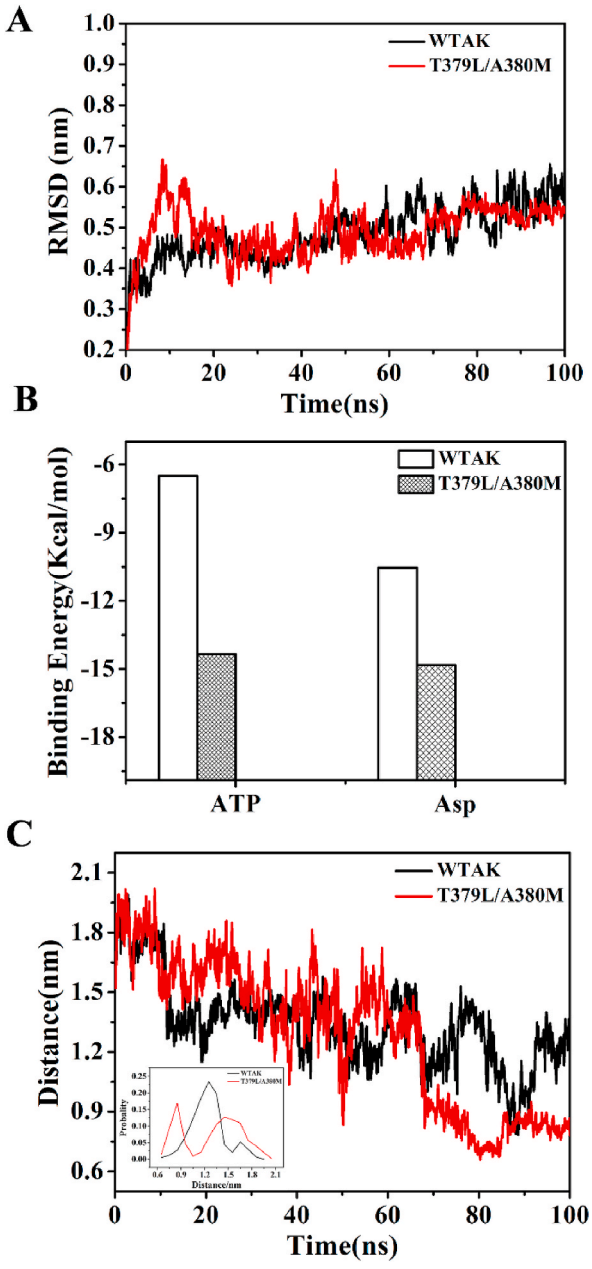

Fig. 5. A, RMSD plot during 100 ns MD simulations. WTAK was represented by black and T379L/A380 M was represented by red, the same below. B, Binging energy between Asp and ATP. C, Distance of Asp and ATP during 100 ns MD simulations. (For interpretation of the references to colour in this figure legend, the reader is referred to the Web version of this article.)

and the ATP and Asp binding pocket. The mutation did not increase the flexibility of the overall residual RMSF, as shown in Fig. 7B. According to Fig. 7C and E, residues Ala160-Ala280 and Cys40-Leu80 were located near ATP and Asp, respectively. Therefore, they were studied in detail in a subsequent experiment. RMSD values of residues Cyc40-Leu80 and Ala160-Ala280 were calculated during a 100 ns simulation. As shown in Fig. 7D, the RMSD values of residual Ala160-Ala280 fluctuated slightly, basically remaining at 0.19 nm with the same occurrence probability in the complex systems of WT-AK + Asp + ATP and T379L/A380 M + Asp + ATP. The RMSD value of residual Cyc40-Leu80 (approximately 0.18 nm) also showed the same variation pattern (Fig. 7F), indicating that the mutation did not cause residual fluctuation at the binding pocket of ATP and Asp, that is, the interaction with ATP and Asp was not affected. We speculated that this might be the reason as to why T379L/A380 M enzyme activity was not as high as that of the single mutant T379L or A380 M.

WT-AK was inhibited by Lys, Thr and Met, and the inhibition effect was the strongest under the action of three inhibitors; The inhibition of the mutant T379L/A380 M was weakened, and even had different degrees of activation, which was mainly contributed by

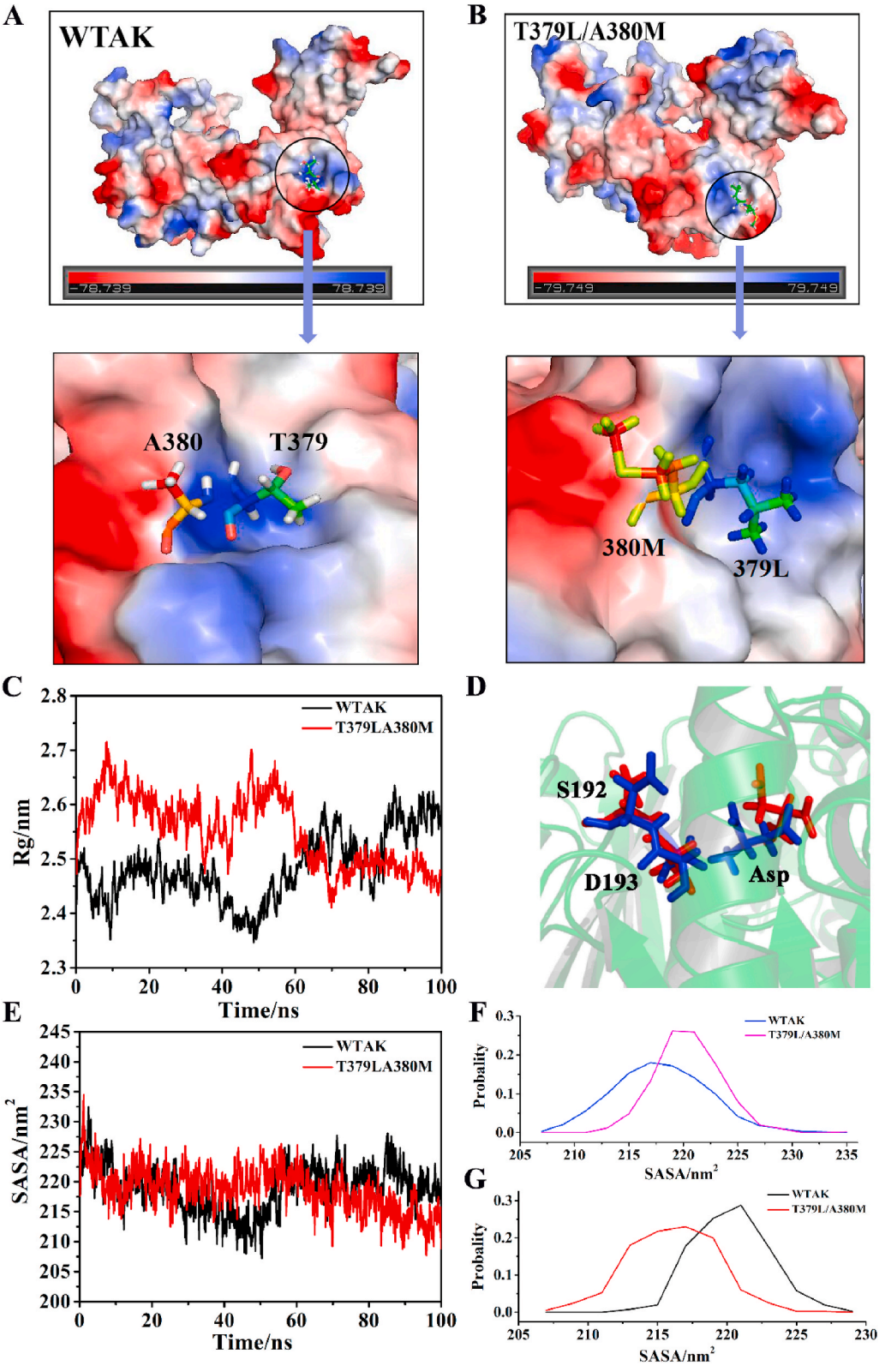

(caption on next page)

Fig. 6. The overall conformation at 100 ns of WTAK (A) and T379L/A380 M (B); C, Radius of gyration plot during 100 ns MD simulations; D, PDB of WTAK and T379L/A380 M were fitted together by software SPDB, representing by the red and blue stick, respectively; E, SASA plot during 100 ns MD simulations; Probability of SASA before 60 ns (F) and after 40 ns (G) during MD simulations. (For interpretation of the references to colour in this figure legend, the reader is referred to the Web version of this article.)

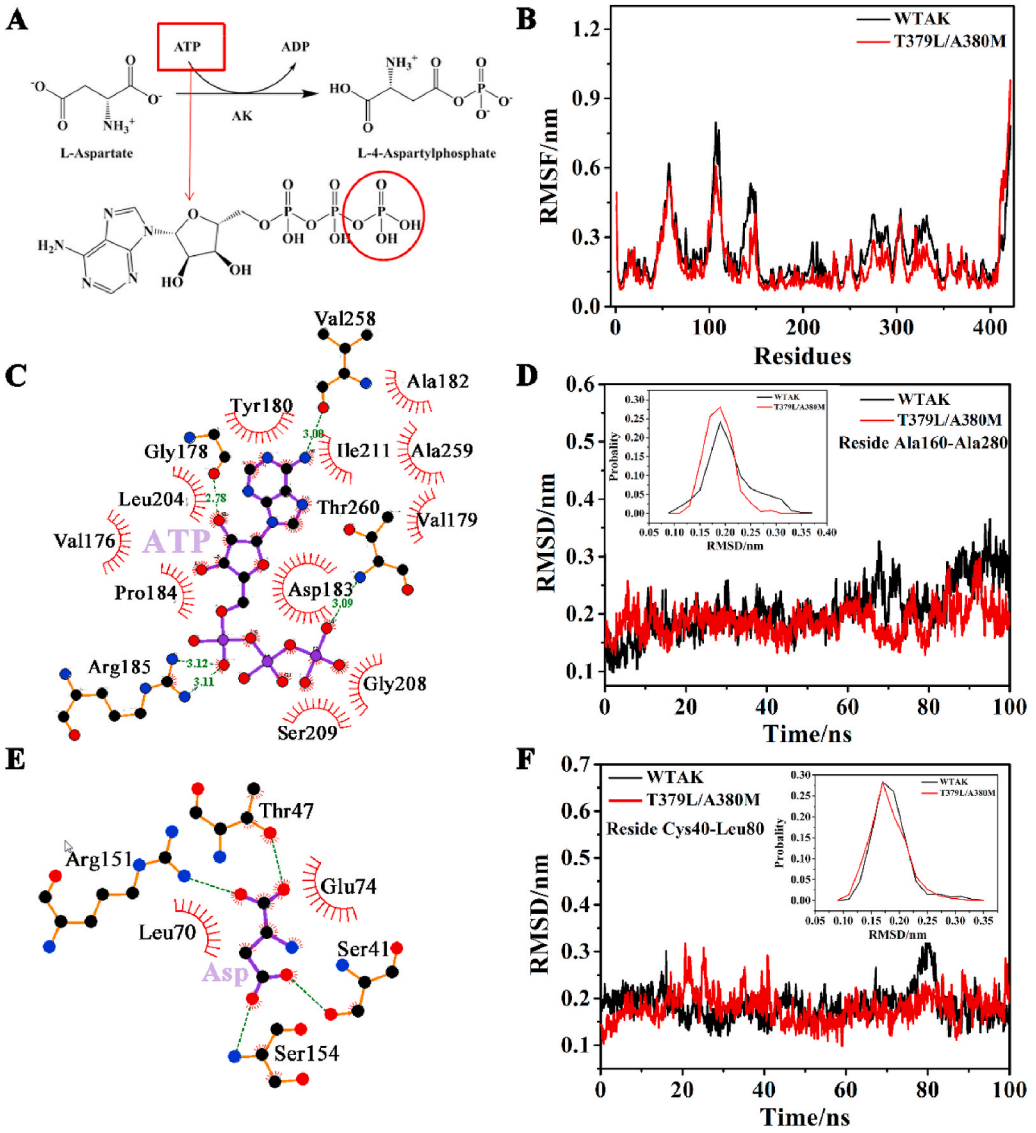

Fig. 7. A, RMSF plot during 100 ns MD simulations. B, The equation of AK catalytic reaction; C, RMSD from residue Ala160-Ala280; D, The residue distribution around ATP; E, RMSD from residue Cys40-Leu80; F, The residue distribution around Asp.

Lys; For example, the mutant T379L/A380 M had different degrees of activation under the action of Lys and Lys + Thr, which might be due to the large changes in the overall spatial conformation caused by the mutations. Site 379 was mutated from the polar amino acid Thr to the non-polar amino acid Leu, and site 380 was mutated from alanine (A) to the sulfur-containing amino acid (M), causing the charge to change from positive to negative (Fig. 7A and B). A study reported that Lys is a competitive inhibitor of Asp [9]. This mutation led to a series of changes, such as a substantial overall conformational change, diminished inhibition, and enhanced affinity for the substrate, and as a result, Lys could not compete with Asp. Thus, it changed from an allosteric inhibitor to an allosteric activator at certain concentrations, which was found to have an important role in activation. However, the associated mechanism of action is still unclear, which is expected to be studied further.

4. Conclusion

The double mutant strain, T379L/A380 M, was obtained, through saturation site-directed mutagenesis and high-throughput screening in this study, and its kinetics and enzymatic properties were characterized. Compared with those of WT-AK, the enzyme activity was increased by 2.74-fold and the enzymatic properties showed that the optimal temperature of T379L/A380 M increased from 26 °C (WT-AK) to 45 °C, the optimal pH changed from 8.0 (WT-AK) to 7.5, and the half-life was reduced from 4.5 to 3.32 h. The inhibitor (Lys) had a good release effect, and the enzyme activity and enzymatic properties were improved. At an experimental level, MST results could explain the reasons for the release of the inhibitory effect and the increase in enzyme activity, and from a simulation level, MD revealed the mechanism through which enzyme activity was improved.

Declarations

Credit author statement

Zhijie Chen: Performed the experiments; Wrote the paper. Yu Fu: Performed the experiments.Shimeng Liu, Xinyu Huang, Xiaoting Kong, Zhaojie Mao, Ning Hu: Analyzed and interpreted the data.Fengxiang Zhang: Conceived and designed the experiments.Caijing Han: Conceived and designed the experiments; Contributed reagents, materials, analysis tools or data; Wrote the paper.

Funding statement

Dr. Caijing Han was supported by Natural Science Foundation of Shandong Province [No. ZR2020QC217] , Shandong Provincial Youth Innovation Team Development Plan of Universities (No. 2019-6-156, Lu-Jiao) , the Domestic Visiting Program of Weifang Medical University and the Doctoral Research Start-up Funds of Weifang Medical University.

Data availability statement

Data included in article/supp. Material/referenced in article.

Declaration of competing interest

The authors declare that they have no known competing financial interests or personal relationships that could have appeared to influence the work reported in this paper.

Acknowledgements

We would also like to thank the Public Health Testing Center of the Weifang Medical University and Weifang Key Laboratory for Food Nutrition and Safety for providing us with the experimental platform and technical guidance.

Appendix A. Supplementary data

Supplementary data related to this article can be found at https://doi.org/10.1016/j.heliyon.2023.e13133.

References

[1] X.L. Tang, X.Y. Du, L.J. Chen, Z.Q. Liu, Y.G. Zheng, Enhanced production of L-methionine in engineered Escherichia coli with efficient supply of one carbon unit, Biotechnol. Lett. 42 (2020) 429–436.
[2] Q. Sheng, X.Y. Wu, X. Xu, X. Tan, Z. Li, B. Zhang, Production of l-glutamate family amino acids in Corynebacterium glutamicum: physiological mechanism, genetic modulation, and prospects, Synth Syst Biotechnol 6 (2021) 302–325.
[3] J. Yang, Y. Lu, Y. Zhao, Z. Bai, Z. Ma, Y. Deng, Site-directed mutation to improve the enzymatic activity of 5-carboxy-2-pentenoyl-CoA reductase for enhancing adipic acid biosynthesis, Enzym. Microb. Technol. 125 (2019) 6–12.
[4] A. Ali, M.W. Azam, A.U. Khan, Non-active site mutation (Q123A) in New Delhi metallo-beta-lactamase (NDM-1) enhanced its enzyme activity, Int. J. Biol. Macromol. 112 (2018) 1272–1277.
[5] A. Yoshida, T. Tomita, T. Kuzuyama, M. Nishiyama, Mechanism of concerted inhibition of alpha2beta2-type hetero-oligomeric aspartate kinase from Corynebacterium glutamicum, J. Biol. Chem. 285 (2010) 27477–27486.
[6] A. Yoshida, T. Tomita, H. Kono, S. Fushinobu, T. Kuzuyama, M. Nishiyama, Crystal structures of the regulatory subunit of Thr-sensitive aspartate kinase from Thermus thermophilus, FEBS J. 276 (2009) 3124–3136.
[7] L. Schuldt, R. Suchowersky, K. Veith, J. Mueller-Dieckmann, M.S. Weiss, Cloning, expression, purification, crystallization and preliminary X-ray diffraction analysis of the regulatory domain of aspartokinase (Rv3709c) from Mycobacterium tuberculosis, Acta Crystallogr., Sect. F: Struct. Biol. Cryst. Commun. 67 (2011) 380–385.
[8] A.Y. Robin, D. Cobessi, G. Curien, M. Robert-Genthon, J.L. Ferrer, R. Dumas, A new mode of dimerization of allosteric enzymes with ACT domains revealed by the crystal structure of the aspartate kinase from Cyanobacteria, J. Mol. Biol. 399 (2010) 283–293.
[9] A. Yoshida, T. Tomita, T. Kurihara, S. Fushinobu, T. Kuzuyama, M. Nishiyama, Structural Insight into concerted inhibition of alpha 2 beta 2-type aspartate kinase from Corynebacterium glutamicum, J. Mol. Biol. 368 (2007) 521–536.

[10] C. Han, L. Fang, C. Liu, Y. Gao, W. Min, Construction of novel aspartokinase mutant A380I and its characterization by molecular dynamics simulation, Molecules (2018) 23.
[11] C. Han, S. Liu, C. Liu, X. Xie, L. Fang, W. Min, The mutant T379L of novel aspartokinase from Corynebacterium pekinense: a combined experimental and molecular dynamics simulation study, Process Biochem. 83 (2019) 77–85.
[12] Z. Fan, L. Fang, L. Wu, Z. Wang, Y. Wang, C. Han, X. Liu, Improved catalytic activity of a novel aspartate kinase by site-directed saturation mutagenesis, Bioproc. Biosyst. Eng. 45 (2022) 541–551.
[13] X. Liu, C. Han, L. Fang, Z. Fan, Y. Wang, X. Gao, J. Shi, W. Min, Mechanism of the feedback-inhibition resistance in aspartate kinase of Corynebacterium pekinense: from experiment to MD simulations, RSC Adv. 11 (2020) 30–38.
[14] S. Isogai, H. Takagi, Enhancement of lysine biosynthesis confers high-temperature stress tolerance to Escherichia coli cells, Appl. Microbiol. Biotechnol. 105 (2021) 6899–6908.
[15] J.Y. Wang, Z.M. Rao, J.Z. Xu, W.G. Zhang, Enhancing beta-alanine production from glucose in genetically modified Corynebacterium glutamicum by metabolic pathway engineering, Appl. Microbiol. Biotechnol. 105 (2021) 9153–9166.
[16] S. Chen, Y. He, Y. Geng, Z. Wang, L. Han, W. Han, Molecular dynamic simulations of bromodomain and extra-terminal protein 4 bonded to potent inhibitors, Molecules 27 (2021).
[17] K. Liu, M. Wang, Y. Zhou, H. Wang, Y. Liu, L. Han, W. Han, Exploration of the cofactor specificity of wild-type phosphite dehydrogenase and its mutant using molecular dynamics simulations, RSC Adv. 11 (2021) 14527–14533.
[18] F. Zheng, T. Tu, X. Wang, Y. Wang, R. Ma, X. Su, X. Xie, B. Yao, H. Luo, Enhancing the catalytic activity of a novel GH5 cellulase GtCel5 from Gloeophyllum trabeum CBS 900.73 by site-directed mutagenesis on loop 6, Biotechnol. Biofuels 11 (2018) 76.
[19] B.A. Manjasetty, M.R. Chance, S.K. Burley, S. Panjikar, S.C. Almo, Crystal structure of Clostridium acetobutylicum Aspartate kinase (CaAK): an important allosteric enzyme for amino acids production, Biotechnol Rep (Amst) 3 (2014) 73–85.
[20] C.C. Li, M.J. Yang, L. Liu, T. Li, C.T. Peng, L.H. He, Y.J. Song, Y.B. Zhu, Y.L. Shen, J. Yang, N.L. Zhao, C. Zhao, Q.X. Zhou, H. Li, M. Kang, A.P. Tong, H. Tang, R. Bao, Mechanistic insights into the allosteric regulation of Pseudomonas aeruginosa aspartate kinase, Biochem. J. 475 (2018) 1107–1119.